J Mater Sci: Mater Med (2008) 19:103–110
DOI 10.1007/s10856-007-3156-9

Synthesis of carbonated hydroxyapatite nanospheres through nanoemulsion

W. Y. Zhou · M. Wang · W. L. Cheung · B. C. Guo · D. M. Jia

Received: 27 March 2006 / Accepted: 22 August 2006 / Published online: 19 June 2007

Abstract This study investigated the nanoemulsion technique as a means to synthesize carbonated hydroxyapatite (CHAp) nanospheres which could be used to produce composite tissue engineering scaffolds. CHAp nanospheres were successfully synthesized by mixing an acetone solution of $Ca(NO_3)_2 \cdot 4H_2O$ with an aqueous solution of $(NH_4)_2HPO_4$ and NH_4HCO_3. Four reaction temperatures, namely, 4, 25, 37 and 55 °C, were investigated and no surfactant was added in all nanoemulsion processes. Wet slurries of CHAp from the nanoemulsions were freeze-dried to obtain dry powders. X-ray diffraction (XRD) results showed that the as-synthesized CHAp nanoparticles were mainly in an amorphous state. After calcination at 900 °C, the apatite became well crystallized. Fourier transform infrared (FTIR) spectroscopy showed that the CHAp was B-type substitution. Both scanning electron microscopy (SEM) and transmission electron microscopy (TEM) revealed that the CHAp particles were spherical in shape and that their sizes were in the nanometer range. The successful synthesis of CHAp nanospheres is a critical step forward in our efforts to fabricate bone tissue engineering scaffolds using the selective laser sintering technology.

W. Y. Zhou · M. Wang · W. L. Cheung (✉)
Department of Mechanical Engineering, The University of Hong Kong, Pokfulam Road, Hong Kong, Hong Kong, China
e-mail: wlcheung@hku.hk

B. C. Guo · D. M. Jia
Department of Polymer Materials and Engineering, South China University of Technology, Guangzhou 510640, China

Introduction

Nanoemulsions, similar to microemulsions, are a new class of emulsions having very fine and uniform droplet sizes, typically in the range of 20–200 nm [1]. Like microemulsions, nanoemulsions can be either transparent or translucent. Some nanoemulsions appear milky with droplet sizes up to 500 nm. Nanoemulsions, in contrast to microemulsions, are not thermodynamically stable but highly kinetically stable because of their small droplet sizes which make them stable against sedimentation and creaming [2]. One major disadvantage of microemulsions is that they require larger amounts of surfactants (typically over 20 wt%) to form than conventional emulsions. This can pose problems for the development of new biomaterials when one considers to meet the paramount requirement of biocompatibility. On the other hand, nanoemulsions offer the possibility of obtaining microemulsion-like dispersions without the need to use high surfactant concentrations or even without the use of any surfactant at all. Nanoemulsions have already found diverse applications in the chemical, cosmetic, pharmaceutical and other industries [3].

Nanoemulsions can be prepared by spontaneous low-energy emulsification at constant temperature [4, 5], the phase inversion temperature (PIT) concept [6], or by the use of a high shear device such as a high pressure homogenizer (aided by appropriate surfactants and cosurfactants). The latter allows a better control of the droplet size and also a large choice of compositions. The polymer nanoprecipitation method firstly described by Fessi et al. [7] is one of the spontaneous low-energy emulsification techniques for nanoemulsion formulation which has these distinctive advantages: (a) the use of potentially toxic components (such as chlorinated solvents)

can be minimized or avoided; and (b) reproducible nanoparticle size with a narrow size distribution can be achieved without an external energy source. The principle of this method resides in the fact that a preformed material can precipitate as nanospheres when a solution in a water-miscible organic solvent (the organic phase) is mixed with water containing surfactants (the aqueous phase). Nanoemulsion has since been considered to be an ideal nanoreactor for the production of metallic nanoparticles such as GeO_2 [8] and CdS [9]. Recently, monodispersed SiO_2 nanoparticles were produced from water-in-oil nanoemulsions by hydrolysis and condensation of ceramic alkoxides into aqueous droplets [10].

Hydroxyapatite (HAp, $Ca_{10}(PO_4)_6(OH)_2$) has attracted much attention because it has extensive applications as bone substituting material due to its similarity, chemically and structurally, to the mineral portion of bone [11]. Conventionally, HAp powders are synthesized using various methods based on dry processes such as solid-state reaction [12] or wet processes such as hydrolysis of calcium phosphates [13] and the precipitation method [14]. Microemulsion has been shown to be one of the few techniques which could be used to synthesize fine HAp particles with smaller size and higher surface area [15]. One major disadvantage of this route, as stated previously, is the required use of large amounts of surfactants and cosurfactants. Nanoemulsions can eliminate this problem. Among various HAp-based bioceramics, carbonated hydroxyapatite (CHAp) is a promising material for bone substitution as it is bioresorbable and also more bioactive in vivo than stoichiometric HAp. CHAp is used mostly as powders and its usefulness depends on the powder properties such as mean particle size, surface area, and morphology. Nanostructured CHAp particles with a high surface area are desirable for their use in many fields including tissue engineering. The synthesis of nano-CHAp was mostly based on the precipitation reaction developed by Nelson and Featherstone [16] and studied in details by Barralet et al. [17–19]. Doi et al. have also successfully produced sintered CHAp which can be resorbed by osteoclasts both under in vitro and in vivo conditions, whereas sintered stoichiometric HAp cannot be resorbed [20–22]. In developing bioactive composites (porous or non-porous) for human tissue repair, apart from particle size and size distribution, the shape of the bioactive and reinforcing particles for the composite is also important [23]. For theoretical analysis of mechanical behavior of a particulate bioceramic-polymer composite, the bioceramic particles in the composite are normally assumed to have a spherical shape. The nanoemulsion method can produce spherical nanoparticles [24]. The synthesis of nano-sized CHAp particles of the preferred spherical shape is a critical step in our efforts to develop composite scaffolds for bone tissue engineering. The aim of the current study was to investigate the use of oil-in-water (O/W) nanoemulsion reactor to synthesize CHAp nanospheres with controlled size which would be used subsequently for constructing composite tissue engineering scaffolds.

Materials and methods

CHAp nanospheres were synthesized using analytical grade $Ca(NO_3)_2 \cdot 4H_2O$, $(NH_4)_2HPO_4$ and NH_4HCO_3 (Uni-Chem, Orientalab, China). The solvent used for making nanoemulsions was analytical grade acetone. The synthesis process is illustrated in Fig. 1. An acetone solution of $Ca(NO_3)_2 \cdot 4H_2O$ was mixed with an aqueous solution of $(NH_4)_2HPO_4$ and NH_4HCO_3 at a molar ratio of Ca^{2+}:PO_4^{3-}:CO_3^{2-} = 1.67:1:0.5 using a magnetic stirrer. The aqueous solution was adjusted to pH 11 with sodium hydroxide (1 M) prior to mixing. All the synthesis work was conducted at temperatures of 4, 25, 37 or 55 °C (which is below the boiling point of acetone of 56.3 °C), respectively, and the mixed solutions were stirred for 0.5 min only. No surfactant was used in all synthesis processes. The resultant nanoprecipitates in the solutions were immediately filtered using a Millipore all-glass vacuum filtration set to avoid particle agglomeration and then washed three times using ultra-pure deionized water. Finally, the slurry of nanoprecipitates was freeze-dried using a Labconco FreeZone freeze-drying system to obtain dry powder. A small quantity of the dry powder synthesized at 25 °C was also calcined at 900 °C for 4 h in air using a Carbolite HTF 18/8 high temperature furnace.

The phase purity and crystallinity of apatite powders produced were examined using X-ray diffraction (Raguku Model D/max III diffractometer, Japan). The X-ray beam

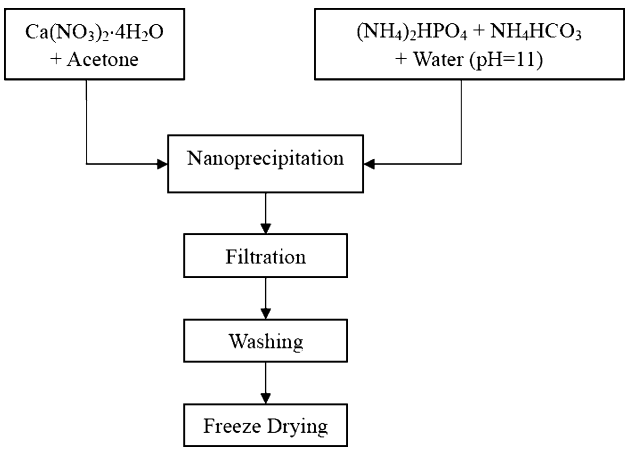

Fig. 1 Process for the synthesis of nano-sized CHAp spheres using the O/W nanoemulsion technique

was nickel-filtered $CuK\alpha_1$ radiation ($\lambda = 0.1540$ nm, operating at 40 kV and 30 mA). XRD data were collected from 20° to 40° (2θ) at a scanning rate of 2°/min. Fourier transform infrared spectroscopy (FTIR, Bruker Vector 33, USA) was performed to determine the presence of functional groups such as OH^- groups and CO_3^{2-} groups in partially substituted apatite.

The morphology of dried nanoprecipitates was examined using a field emission scanning electron microscope (FE-SEM, LEO 1530, Germany). A transmission electron microscope (TEM, Philips Tecnai 20, the Netherlands) with an energy dispersive X-ray spectrometry attachment (EDX, Inca 300, UK) was also used to study the morphology, surface and fine crystalline structure of dried nanoprecipitates. TEM samples were prepared by ultrasonically dispersing the powders in acetone prior to their collection on carbon-coated copper grids. The mean particle size of nanoprecipitates was estimated from TEM dark field images. Selected area electron diffraction (SAD) patterns were also taken in order to confirm the amorphous or crystalline nature as well as composition of the powders. The specific surface area of apatite powders was measured using the BET method (Micromeritics, ASAP 2010 N, USA).

Results

Nanoemulsion and nanoparticles

As shown in Fig. 2, the nanoemulsions prepared in the current study appeared slightly milky. The tinge of white color increased with increasing nanoprecipitate content. Due to the characteristics of nanoemulsion, the translucent solutions prepared in the nanoemulsion process possessed good stability against sedimentation. The as-synthesized nanoparticles before and after freeze-drying are shown in Fig. 3. The freeze-dried powders, as shown in Fig. 3B, could flow easily. It appeared that the degree of agglomeration caused by this nanoemulsion and freeze-drying technique is comparatively lower than the wet precipitation and conventional oven drying method which tends to give large agglomerates.

Fig. 2 CHAp nanoemulsion (*left*) as compared to pure water (*right*)

Identification of carbonated hydroxyapatite (CHAp)

Figure 4 displays XRD patterns of nanoparticles that were synthesized at different temperatures (4, 25, 37 and 55 °C, respectively). All diffraction patterns of samples A to D had a very broad hump, indicating the nearly amorphous nature or the very low degree of crystallinity of the nanoparticles. It appeared that the reaction temperature had not affected the crystallinity of particles synthesized through

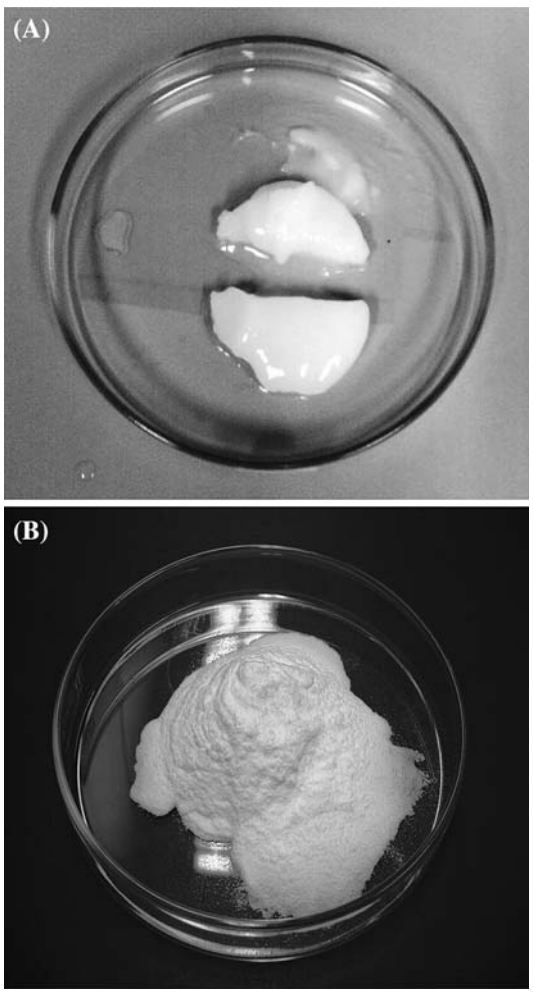

Fig. 3 As-synthesized nanoparticles: (**A**) wet slurry before freeze-drying, (**B**) dry powder after freeze-drying

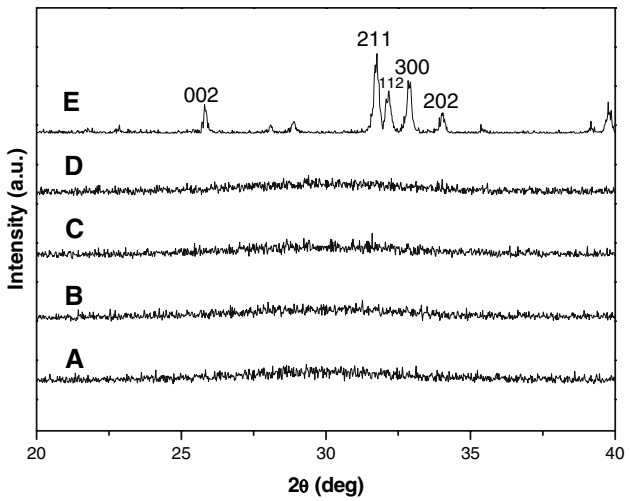

Fig. 4 XRD patterns of CHAp nanoparticles synthesized at: (A) 4 °C, (B) 25 °C, (C) 37 °C, (D) 55 °C, (E) synthesized at 25 °C and calcined at 900 °C for 4 h in air

nanoemulsion. For comparison, the XRD pattern of calcined particles (sample E) is included in Fig. 4, which exhibited sharp peaks of crystalline HAp (JCPDS 9-432). The XRD results obtained from the calcined powders suggest that the nanoparticles synthesized at the different temperatures were hydroxyapatite (HAp).

Figure 5 exhibits the FTIR spectra of the nanoparticles synthesized at room temperature before and after calcination at 900 °C, with the bands being labeled accordingly for different functional groups. In both spectra, bands for OH^- and PO_4^{3-} groups were present. Small amount of occluded water gave rise to a band at 1,647 cm^{-1} in the spectrum of the as-synthesized nanoparticles. The spectrum for the as-synthesized nanoparticles exhibited bands for the

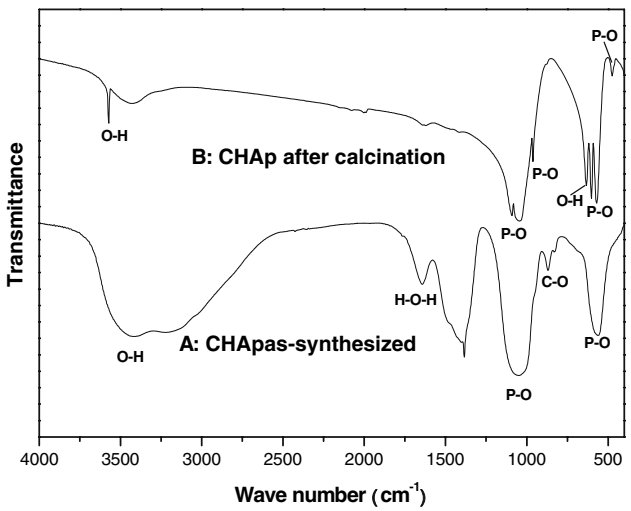

Fig. 5 FTIR spectra of carbonated hydroxyapatite: (*A*) synthesized at 25 °C, (*B*) synthesized at 25 °C and calcined at 900 °C for 4 h in air

CO_3^{2-} group at 870 cm^{-1} and 1,467–1,412 cm^{-1}, these bands disappeared from the spectrum obtained from the calcined powder. FTIR analysis indicates that the apatite synthesized through nanoemulsion had CO_3^{2-} substitutions and hence the powders were carbonated hydroxyapatite (CHAp).

Morphology and characteristics of CHAp nanospheres

FE-SEM micrographs of the as-synthesized and the synthesized and calcined CHAp powders are shown in Figs. 6 and 7, respectively. The as-synthesized CHAp powders (Fig. 6) were tiny agglomerates of nanoparticles (~20 nm in diameter) in the freeze-dried state whereas the calcined CHAp powders (Fig. 7) exhibited particles that had coarsened to sizes in the micrometer range. The SEM micrograph shown as Fig. 7 depicts CHAp particles that had even undergone necking at the high temperature due to the high-temperature calcination of the highly reactive nano-sized crystals. This observation was reflected by the surface area measurements of CHAp powders (Table 1).

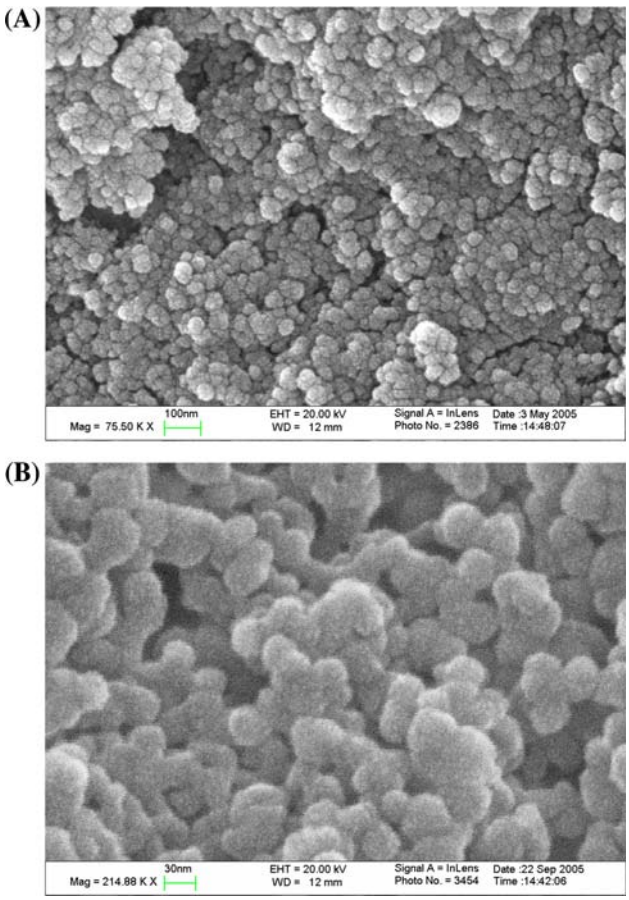

Fig. 6 Morphology of CHAp nanospheres synthesized at 25 °C: (**A**) low magnification (scale bar 100 nm), (**B**) high magnification (scale bar 30 nm)

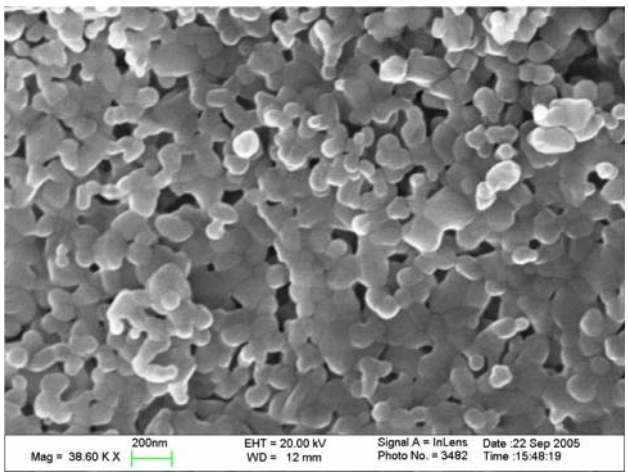

Fig. 7 Morphology of CHAp powder synthesized at 25 °C and calcined at 900 °C for 4 h in air (scale bar 200 nm)

Table 1 BET specific surface area of CHAp powders

State of powder	BET specific surface area (m^2/g)
CHAp synthesized at 25 °C	43.67 ± 0.03
CHAp synthesized at 25 °C and calcined at 900 °C	13.24 ± 0.09

After calcination at 900 °C, the specific surface area of the CHAp particles decreased from the original value of 43.67 m^2/g for the as-synthesized nanoparticles to 13.24 m^2/g. This is a very large reduction in surface area, which can affect properties and hence the use of CHAp particles synthesized.

Figure 8 is a TEM micrograph, together with the SAD pattern, of the as-synthesized CHAp nanoparticles. Clearly, the as-synthesized nanoparticles were spherical in shape and their sizes were in the range of 10–30 nm. Image analysis of TEM micrographs using the ImagePro® software revealed that these CHAp nanospheres were 16.8 ± 2.6 nm in diameter. The SAD pattern shown in Fig. 8 was obtained from nanosphere agglomerates and exhibited much-diffused electron diffraction rings, indicating a very low degree of crystallinity of the as-synthesized CHAp particles, which agreed well with the XRD results in Fig. 4. Figure 9 shows the EDX spectrum of the as-synthesized CHAp. The Ca/P ratio determined from this spectrum was 1.63, which suggests that the CHAp was calcium-deficient.

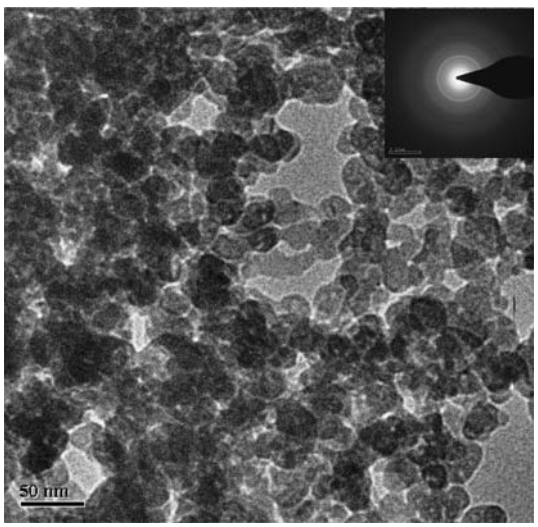

Fig. 8 TEM image and SAD pattern (inset) of the CHAp powder synthesized at 25 °C

Discussion

Acetone and ethanol are two common solvents which can dissolve calcium nitrate 4-hydrate. Liu et al. [25] and Cheng et al. [26] used ethanol as one reaction phase to synthesize HAp in their sol–gel production route. Ethanol is a protic solvent, and when dissolved with calcium nitrate 4-hydrate, ethoxide groups could replace some of the nitrate groups to form $Ca(OEt)_y(NO_3)_{2-y}$ which could be incorporated finally into the apatite structure. In the current study, acetone was chosen as the oil phase because it is a non-protic solvent and thus the solvent would not affect the purity of CHAp synthesized. Meanwhile, acetone is present in very small quantities in normal urine and blood and as a product of the breakdown of body fat [27]. Using acetone as a reaction medium to synthesize apatite also mimics the natural process of apatite formation. In the nanoprecipitation process for polymers, acetone acts as a common solvent due to its ability to dissolve many biodegradable polymers such as poly(D, L-lactide) (PLA), poly(D, L-lactide-co-glycolide) (PLGA) and polycaprolactone (PCL). Combining the CHAp nanoemulsion method reported here with the polymer emulsion solvent evaporation method, acetone can be used as a preparation medium for forming spheres, either in nanometer size or in micrometer size, of bioceramic/biodegradable polymer nanocomposite. Indeed, such composite spheres have been successfully produced using this bioceramic-nanoemulsion-co-polymer-emulsion technique. Figure 10 shows an SEM micrograph of the cross-section of a microsphere of CHAp/PLA nanocomposite with CHAp nanospheres being incorporated into the PLA matrix, which was produced in our current on-going investigation. Further work is being carried out to fabricate bone tissue engineering scaffolds from these composite microspheres using the selective laser sintering (SLS) technology, which has been proven effective in producing porous scaffolds with controlled pore characteristics [28]. The incorporation of nano-sized, amorphous CHAp particles

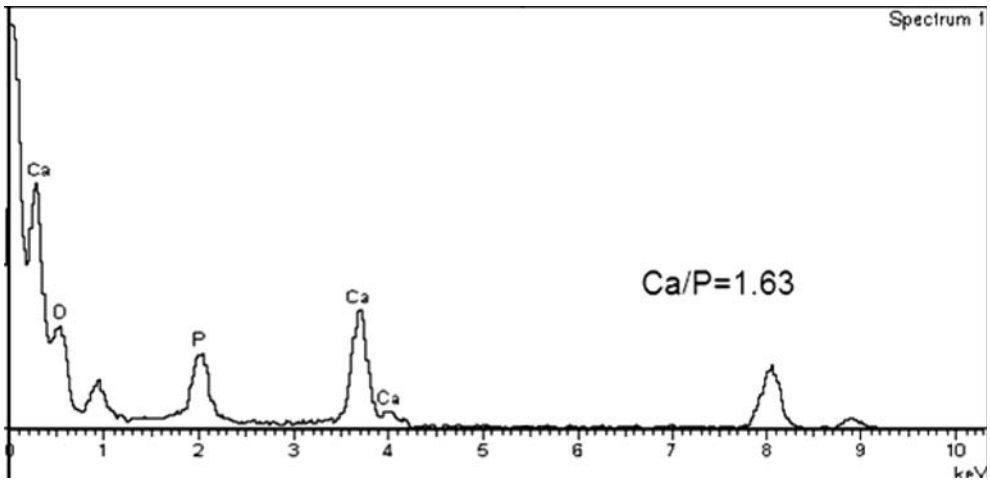

Fig. 9 EDX spectrum of the CHAp powder synthesized at 25 °C

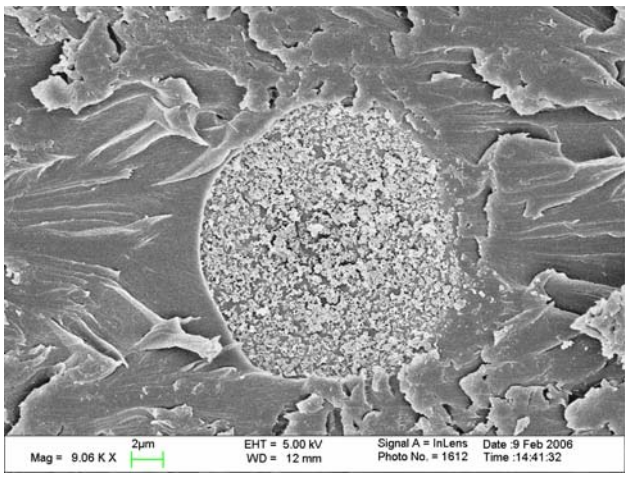

Fig. 10 Cross-sectional view of a microsphere of CHAp/PLA nanocomposite containing 10 wt% of CHAp nanospheres. The CHAp/PLA microsphere (*center*) was embedded in epoxy resin before sectioning with a microtome

in scaffolds is expected to enhance greatly osteoconductivity of the scaffolds in bone tissue engineering.

It has been reported that in the wet synthesis processes, HAp mostly forms needle-shaped crystallites that have preferential growth in the (002) direction [29, 30]. In the current study, the nanoemulsion method produced spherical nanoparticles mainly because the CHAp particles precipitated were confined in nano-sized emulsion droplets. LeGeros and co-workers demonstrated that the CO_3^{2-} in substituted HAp caused changes in the size and shape of apatite crystal: from acicular crystals to rods to equiaxed crystals with an increasing carbonate content from 2.5 to 17.25 wt% [11]. In the current study, the theoretical carbonate content was 12.8 wt% as calculated from the chemical formula $Ca_{10}(PO_4)_4(CO_3)_2(OH)_2$. The formation of spherical CHAp nanoparticles is due to two reasons: one is the relatively high carbonate content in the CHAp structure, which agrees with LeGeros' observation; the other is the nanoemulsion reactor used in the current synthesis process which is caused by the Ouzo effect [31]. The Ouzo effect is a spontaneous emulsification, which causes the formation of acetone/water nanoemulsion. The mechanism of the Ouzo effect is a liquid–liquid nucleation process which arises when mixing with water, the water miscible oil becomes greatly supersaturated, resulting in the nucleation of oil droplets. Following this, the oil immediately begins diffusing to the nearest droplet so that the supersaturation decreases and no further nucleation of droplets occurs. The final metastable emulsion is an ideal nano-reactor to form either ceramic or polymer nanospheres.

As has been observed through XRD analysis (Fig. 4) in the current study, CHAp particles synthesized through nanoemulsion were amorphous or possessed a very low degree of crystallinity and the reaction temperature in the nanoemulsion process did not affect the crystallinity of the CHAp particles. This could probably be due to the immediate filtration after nanoprecipitate formation and the subsequent freeze-drying process. Tadic and co-workers reported similar XRD results when they used high mixing rate and low reaction temperature to form CHAp through a wet precipitation process [32]. Furthermore, carbonate has been known to inhibit HAp crystallization [33]. There are two processes involved in the formation of apatite in the wet synthesis process: first, precipitation from solution in an amorphous state and second, crystallization within the solid. The proportion of these two processes determines the degree of crystallinity of the apatite obtained [32]. In the current study, the second process was prevented by the fast filtration and freeze-drying processes. Therefore, from the XRD results, the overall assessment of the CHAp synthesized is that it was mainly in the amorphous state. However, the crystallization process could not be totally

stopped, and hence the SAD patterns indicated some degree of crystallinity of the CHAp nanoparticles (Fig. 8).

The FTIR spectra shown in Fig. 5 also give some information on the crystallinity of the CHAp particles. Tadic et al. [32] demonstrated in their IR study that the crystallinity of CHAp would affect the phosphate bands at 590–610 cm^{-1} and around 1,000 cm^{-1}. Broad and unresolved bands indicated a poor crystallinity, whereas sharp and splitting peaks at 565/605 and 1,070/1,150 cm^{-1} indicated a high crystallinity. In the current study, on spectrum A in Fig. 5, the absorption bands of $v_3PO_4^{3-}$ and $v_4PO_4^{3-}$ are broad and the bands of $v_1PO_4^{3-}$ and $v_2PO_4^{3-}$ are absent for the as-synthesized CHAp, which indicate the amorphous state of the CHAp. On the issue of CO_3^{2-} substitution in CHAp, the carbonate ions can substitute for both the hydroxyl (A-type CHAp) and phosphate (B-type CHAp) groups in the HAp structure [33]. The band at 870 cm^{-1} is attributed to $v_2CO_3^{2-}$ substituting for phosphate positions in the HAp lattice (i.e., B-type CHAp). The typical peak of the A-type CHAp at 880 cm^{-1} [34] did not appear for the CHAp synthesized in the current study. The double peaks of $v_2CO_3^{2-}$ in 1,467–1,412 cm^{-1} are broad and unresolved, also indicating the amorphous state of the CHAp. On spectrum B in Fig. 5, the absorption bands at 602/571 and 474 cm^{-1} are attributed to $v_4PO_4^{3-}$ and $v_2PO_4^{3-}$ from the calcined, crystalline HAp, respectively. Absorptions at 1,092/1,043 and 962 cm^{-1} are due to $v_3PO_4^{3-}$ and $v_1PO_4^{3-}$. The sharp peaks of O–H stretching and bending at 3,574 and 633 cm^{-1}, respectively, indicate that the material had a high degree of crystallinity. As the calcination temperature used in the current study was high, the peaks of the CO_3^{2-} group totally disappeared from spectrum B, suggesting that the carbonate ion had evolved into CO_2 gas during the calcination process.

The carbonate content in bone mineral is around 4–8 wt% and it has been shown to vary depending on the age of the individual, with an increase of A-type substituted apatite in the old bone [35]. Hence, B-type CHAp is the most abundant apatite in bones of young people. Astala and Stott [36] used the first principles simulations to study the different carbonate substitution mechanisms in bulk HAp. Their results showed that B-type or PO_4^{3-} substitution is energetically preferred to A-type or OH^- substitution. This can probably explain that most CHAp synthesized, reported in the literature as well as found in the current study, is the B-type substituted HAp.

Because no surfactant was used in the nanoemulsion processes of the current study, the specific surface area of CHAp synthesized is not as high as surfactant-aided systems [29]. The calcination temperature selected in the current study was high and hence caused large reductions in the specific surface area of the CHAp particles (Table 1). The purpose of using such a high calcination temperature was to crystallize the nanoparticles in order to demonstrate that the as-synthesized nanoparticles through the nanoemulsion method were actually apatite. However, in post-synthesis treatment of the precipitated CHAp nanospheres for their actual use as a biomaterial on its own or incorporated into other materials, if calcination is required, the calcination temperature should be kept as low as possible in order not to lose the CO_3^{2-} functional group nor to reduce the characteristic high surface area of the nanoparticles.

The high degree of flowability of freeze-dried, as-synthesized CHAp powders is another distinctive feature. This flow property is important when the CHAp powders are used as raw materials to produce non-porous bioceramic/polymer composites or porous composite scaffolds for human tissue repair. The adequate ability of the powders to flow is required so that the nanospheres could be dispersed sufficiently in the matrix polymer, which could be in the molten state or in the state of polymer solutions, thus enabling the eventual achievement of obtaining high performance (both mechanical and biological) biomaterials.

Conclusions

The nanoemulsion technique has been found very promising for the synthesis of nano-sized, B-type CHAp particles in the spherical shape. Acetone is an appropriate oil phase to form the nanoemulsions. The as-synthesized CHAp nanospheres are mainly in the amorphous state and become highly crystalline after calcination at 900 °C. The reaction temperature in nanoemulsion processes does not affect the crystallinity of as-synthesized CHAp nanospheres. The CHAp nanospheres can be used to produce microspheres of CHAp/PLA nanocomposite, which can in turn be utilized to make highly osteoconductive composite scaffolds for bone tissue engineering using the selective laser sintering technology.

Acknowledgments This work was supported by a CERG research grant (HKU 7118/05E) from the Hong Kong Research Grants Council. W. Y. Zhou thanks The University of Hong Kong for providing him with a research studentship.

References

1. C. SOLANS, P. IZQUIERDO, J. NOLLA, N. AZEMAR and M. J. GARCIA-CELMA, *Curr. Opin. Colloid Interface Sci.* **10** (2005) 102
2. N. USON, M. J. GARCIA and C. SOLANS, *Colloids Surf. A Physicochem. Eng. Asp.* **250** (2004) 415
3. P. IZQUIERDO, J. ESQUENA, T. F. TADROS, C. DEDEREN, M. J. GARCIA, N. AZEMAR and C. SOLANS, *Langmuir* **18** (2002) 26

4. A. FORGIARINI, J. ESQUENA, C. GONZALEZ and C. SOLANS, *Langmuir* **17** (2001) 2076
5. K. BOUCHEMAL, S. BRIANCON, E. PERRIER and H. FESSI, *Int. J. Pharm.* **280** (2004) 241
6. P. IZQUIERDO, J. ESQUENA, T. F. TADROS, J. C. DEDEREN, J. FENG, M. J. GARCIA-CELMA, N. AZEMAR and C. SOLANS, *Langmuir* **20** (2004) 6594
7. H. FESSI, F. PUISIEUX, J. P. DEVISSAGUET, N. AMMOURY and S. BENITA, *Int. J. Pharm.* **55** (1989) R1
8. T. KAWAI, Y. USUI and K. KON-NO, *Colloids Surf. A Physicochem. Eng. Asp.* **149** (1999) 39
9. M. L. CURRI, G. LEO, M. ALVISI, A. AGOSTIANO, M. DELLA MONICA and L. VASANELLI, *J. Colloid Interface Sci.* **243** (2001) 165
10. M. PORRAS, A. MARTINEZ, C. SOLANS, C. GONZALEZ and J. M. GUTIERREZ, *Colloids Surf. A Physicochem. Eng. Asp.* **270–271** (2005) 189
11. R. Z. LEGEROS and J. P. LEGEROS, in ''An introduction to bioceramics'', edited by L. L. HENCH and J. WILSON (World Scientific, 1993) p. 139
12. R. R. RAO, H. N. ROOPA and T. S. KANNAN, *J. Mater. Sci. Mater. Med.* **8** (1997) 511
13. K. ISHIKAWA and E. D. EANES, *J. Dent. Res.* **72** (1993) 474
14. E. LANDI, A. TAMPIERI, G. CELOTTI and S. SPRIO, *J. Eur. Ceram. Soc.* **20** (2000) 2377
15. M. UOTA, H. ARAKAWA, N. KITAMURA, T. YOSHIMURA, J. TANAKA and T. KIJIMA, *Langmuir* **21** (2005) 4724
16. D. G. A. NELSON and J. D. B. FEATHERSTONE, *Calcif. Tissue Int.* **34** (1982) S69
17. J. BARRALET, S. BEST and W. BONFIELD, *J. Biomed. Mater. Res.* **41** (1998) 79
18. J. E. BARRALET, S. M. BEST and W. BONFIELD, *J. Mater. Sci. Mater. Med.* **11** (2000) 719
19. J. BARRALET, J. C. KNOWLES, S. BEST and W. BONFIELD, *J. Mater. Sci. Mater. Med.* **13** (2002) 529
20. Y. DOI, T. KODA, N. WAKAMATSU, T. GOTO, H. KAMEMIZU, Y. MORIWAKI, M. ADACHI and Y. SUWA, *J. Dent. Res.* **72** (1993) 1279
21. Y. DOI, H. IWANAGA, T. SHIBUTANI, Y. MORIWAKI and Y. IWAYAMA, *J. Biomed. Mater. Res.* **47** (1999) 424
22. M. HASEGAWA, Y. DOI and A. UCHIDA, *J. Bone Joint Surg. Br.* **85B** (2003) 142
23. M. WANG, *Biomaterials* **24** (2003) 2133
24. M. CHORNY, I. FISHBEIN, H. D. DANENBERG and G. GOLOMB, *J. Control. Release* **83** (2002) 389
25. D.-M. LIU, T. TROCZYNSKI and W. J. TSENG, *Biomaterials* **22** (2001) 1721
26. K. CHENG, G. SHEN, W. WENG, G. HAN, J. M. F. FERREIRA and J. YANG, *Mater. Lett.* **51** (2001) 37
27. D. J. REISMAN, Acetone: first draft (Geneva: World Health Organization, 1998)
28. S. H. LEE, W. Y. ZHOU, W. L. CHEUNG and M. WANG, ''Transactions of the society for biomaterials 30th annual meeting'', (TN, USA: Memphis, 2005) p. 348
29. S. BOSE and S. K. SAHA, *Chem. Mater.* **15** (2003) 4464
30. S. PUAJINDANETR, S. M. BEST and W. BONFIELD, *Br. Ceram. T* **93** (1994) 96
31. F. GANACHAUD and J. L. KATZ, *Chemphyschem* **6** (2005) 209
32. D. TADIC, F. PETERS and M. EPPLE, *Biomaterials* **23** (2002) 2553
33. R. Z. LEGEROS, O. R. TRAUTZ, E. KLEIN and J. P. LEGEROS, *Experientia* **25** (1969) 5
34. E. LANDI, G. CELOTTI, G. LOGROSCINO and A. TAMPIERI, *J. Eur. Ceram. Soc.* **23** (2003) 2931
35. C. REY, V. RENUGOPALAKRISHNAN, B. COLLINS and M. J. GLIMCHER, *Calcif. Tissue Int.* **49** (1991) 251
36. R. ASTALA and M. J. STOTT, *Chem. Mater.* **17** (2005) 4125